

# Assembly of Highly Organized Carbon Nanotube Architectures by Chemical Vapor Deposition

B. Q. Wei,<sup>†</sup> R. Vajtai,<sup>†</sup> Y. Jung,<sup>†</sup> J. Ward,<sup>†</sup> R. Zhang,<sup>‡</sup> G. Ramanath,<sup>\*,†</sup> and P. M. Ajayan<sup>\*,†</sup>

Materials Science & Engineering Department, Rensselaer Polytechnic Institute, Troy, New York 12180, and Physical Sciences Research Laboratories, Motorola Labs, 7700 South River Parkway, Tempe, Arizona 85284

Received March 19, 2002. Revised Manuscript Received December 6, 2002

Controllable assembly of ordered nanoscale structural units in geometrically well-defined configurations is essential for building integrated nanoscale systems. Here, we describe a powerful method to simultaneously grow aligned carbon nanotube bundles in multiple, predetermined orientations on planar substrates to build one- to three-dimensional architectures. We effect multidirectional nanotube growth by gas-phase delivery of a xylene-ferrocene mixture on to lithographically machined silica surface templates. The preference of nanotubes to grow normal to, and selectively on, silica surfaces forces the nanotubes to inherit the topography of the substrate templates, enabling premeditated selection of both nucleation sites and growth direction. By using silica templates of different shapes, we can build a wide variety of organized nanotube structures of differing complexity and shapes, density, dimensions, and orientation, for example, mutually orthogonal arrays of pillars and platelets, films with hierarchical pores, and free-standing membranes. This fabrication route is scalable to large areas and compatible with silicon microfabrication technology and opens up attractive possibilities for constructing nanotube architectures for applications such as electronic switching, electromechanical actuation, and fluidic separation.

## 1. Introduction

Future devices consisting of organized structures, of various functional materials with new and exciting properties, will be built from nanoscale building blocks.<sup>1–3</sup> These nanoscale building blocks can be produced by a variety of synthesis routes,<sup>4–8</sup> and novel properties arising from their low dimensionality and electronic structure are known for a wide range of materials. However, the know-how for creating hierarchical structures by organizing nanostructural units, important for fabricating integrated devices, is currently lacking. Carbon nanotube is one such material, which promises to have a wide range of applications.<sup>9–11</sup> But there is only limited knowledge available to controllably build

organized architectures with predetermined orientations. Thus far, vertically aligned nanotubes have been fabricated on catalyst-printed planar substrates by chemical vapor deposition (CVD) by several researchers.<sup>12–18</sup> Recent works have shown that nanotubes can be aligned in horizontal configurations through electric fields or microfluidic forces.<sup>19–21</sup>

\* Corresponding authors. E-mail: Ramanath@rpi.edu (G. Ramanath); Ajayan@rpi.edu (P. M. Ajayan).

<sup>†</sup> Rensselaer Polytechnic Institute.

<sup>‡</sup> Motorola Labs.

(1) Duan, X. F.; Huang, Y.; Cui, Y.; Wang, J. F.; Lieber, C. M. *Nature* **2001**, *409*, 66–69.

(2) Mirkin, C. A. *Inorg. Chem.* **2000**, *39*, 2258–2272.

(3) Alivisatos, A. P.; Barbara, P. F.; Castleman, A. W.; Chang, J.; Dixon, D. A.; Klein, M. L.; McLendon, G. L.; Miller, J. S.; Ratner, M. A.; Rosky, P. J.; Stupp, S. I.; Thompson, M. E. *Adv. Mater.* **1998**, *10*, 1297–1336.

(4) Boal, A. K.; Ilhan, F.; DeRouchey, J. E.; Thurn-Albrecht, T.; Russell, T. P.; Rotello, V. M. *Nature* **2000**, *404*, 746–748.

(5) Coronado, E.; Galan-Mascaros, J. R.; Gomez-Garcia, C. J.; Laukhin, V. *Nature* **2000**, *408*, 447–449.

(6) Cui, Y.; Lieber, C. M. *Science* **2001**, *291*, 851–853.

(7) Yang, H.; Coombs, N.; Sokolov, I.; Ozin, G. A. *Nature* **1996**, *381*, 589–592.

(8) McConnell, W. P.; Novak, J. P.; Brousseau, L. C.; Fuierer, R. R.; Tenent, R. C.; Feldheim, D. L. *J. Phys. Chem. B* **2000**, *104*, 8925–8930.

(9) Dresselhaus, M. S.; Dresselhaus, G.; Avouris, P. *Carbon nanotubes: synthesis, structure, properties, and applications*; Springer: Berlin, 2001.

(10) Dekker, C. *Phys. Today* **1999**, *52*, 22–28.

(11) Yakobson, B. I.; Smalley, R. E. *Am. Sci.* **1997**, *85*, 324–337.

(12) Li, W. Z.; Xie, S. S.; Qian, L. X.; Chang, B. H.; Zou, B. S.; Zhou, W. Y.; Zhao, R. A.; Wang, G. *Science* **1996**, *274*, 1701–1703.

(13) Sen, R.; Govindaraj, A.; Rao, C. N. R. *Chem. Phys. Lett.* **1997**, *267*, 276–280.

(14) Terrones, M.; Grobert, N.; Olivares, J.; Zhang, J. P.; Terrones, H.; Kordatos, K.; Hsu, W. K.; Hare, J. P.; Townsend, P. D.; Prassides, K.; Cheetham, A. K.; Kroto, H. W.; Walton, D. R. M. *Nature* **1997**, *388*, 52–55.

(15) Ren, Z. F.; Huang, Z. P.; Xu, J. W.; Wang, J. H.; Bush, P.; Siegal, M. P.; Provencio, P. N. *Science* **1998**, *282*, 1105–1107.

(16) Fan, S. S.; Chapline, M. G.; Franklin, N. R.; Tomblor, T. W.; Cassell, A. M.; Dai, H. J. *Science* **1999**, *283*, 512–514.

(17) Kind, H.; Bonard, J. M.; Emmenegger, C.; Nilsson, L. O.; Hernadi, K.; Maillard-Schaller, E.; Schlappbach, L.; Forro, L.; Kern, K. *Adv. Mater.* **1999**, *11*, 1285–1289.

(18) Schlittler, R. R.; Seo, J. W.; Gimzewski, J. K.; Durkan, C.; Saifullah, M. S. M.; Welland, M. E. *Science* **2001**, *292*, 1136–1139.

(19) Zhang, Y. G.; Chang, A. L.; Cao, J.; Wang, Q.; Kim, W.; Li, Y. M.; Morris, N.; Yenilmez, E.; Kong, J.; Dai, H. J. *Appl. Phys. Lett.* **2001**, *79*, 3155–3157.

(20) Star, A.; Stoddart, J. F.; Steurman, D.; Diehl, M.; Boukai, A.; Wong, E. W.; Yang, X.; Chung, S. W.; Choi, H.; Heath, J. R. *Angew. Chem. Int. Ed.* **2001**, *40*, 1721–1725.

(21) Rueckes, T.; Kim, K.; Joselevich, E.; Tseng, G. Y.; Cheung, C. L.; Lieber, C. M. *Science* **2000**, *289*, 94–97.

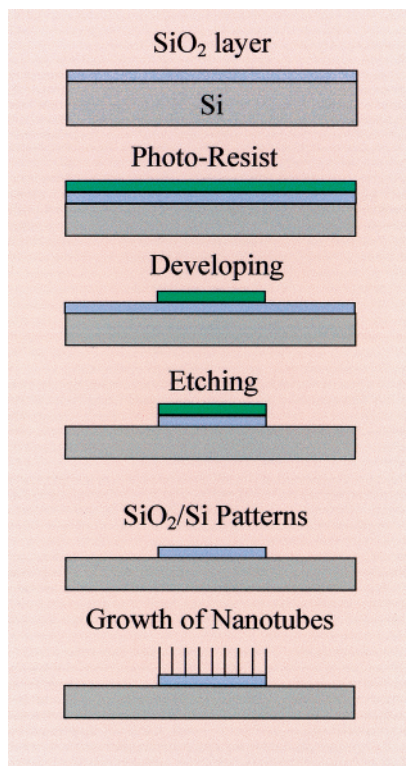


**Figure 1.** Schematic sketch of the process used to create silica patterns on a silicon substrate. The sequence from top to bottom is as follows: generation of a SiO<sub>2</sub> layer on a Si wafer by thermal oxidation or PECVD; spin coating of a photoresist; photoexposure through a mask and resist development; etching the exposed SiO<sub>2</sub>; photoresist removal and growth of nanotubes on patterned SiO<sub>2</sub>.

Here, we show the simultaneous growth of aligned nanotubes in any sets of predetermined, multiple directions, in a single-process step. The level of control provided by this method enables us to construct complex nanotube-based architectures, which could lead to nanotube-based devices and systems in a scalable fashion.

## 2. Experimental Details

All the nanotube structures are designed and built on nonplanar patterns composed of SiO<sub>2</sub> and Si surfaces. The substrates used in this study were Si(100) wafers capped with 100-nm-thick silica. In some cases thicker silica layers (up to ~8.5 μm) were deposited by plasma-enhanced chemical vapor deposition (PECVD) to create high-aspect-ratio silica features. Patterns of Si/SiO<sub>2</sub> of various shapes were generated by photolithography followed by a combination of wet and/or dry etching. A schematic sketch of the lithography procedure is shown in Figure 1.

The nanotubes were grown in a CVD tube furnace system (see Figure 2) from a vapor-phase mixture of xylene [C<sub>8</sub>H<sub>10</sub>] and ferrocene [Fe(C<sub>5</sub>H<sub>5</sub>)<sub>2</sub>]. A 0.01 g/mL solution of ferrocene in xylene was preheated at about 150 °C and sublimed into the CVD chamber. Prior to this, the chamber was pumped to a 10<sup>-3</sup> Torr vacuum, backfilled with flowing argon to ~100 mTorr and heated gradually to 800 °C. Under our growth conditions ferrocene is the nanotube nucleation initiator and xylene the carbon source. This precursor combination results in the *selective* growth of 20–30-nm-diameter multiwalled carbon nanotubes on SiO<sub>2</sub> surfaces as demonstrated earlier.<sup>22,23</sup> No nanotube growth is observed on pristine Si surfaces or on the native oxide layer. The growth rate is ~10 μm/min and micrometer-thick films comprised of vertically aligned nanotubes can be produced on planar silica substrates in a few minutes.<sup>22</sup> The average center-to-center spacing between adjacent nanotubes in these films is ~50 nm.<sup>24</sup>

The growth morphology, structure, and properties of the nanotubes grown were investigated and characterized with scanning and transmission electron microscopy. SEM measurements were carried out in a JEOL JSM-6330F microscope equipped with a field emission gun operated at 5 keV. A Renishaw S 2000 Raman spectroscope using an argon-ion laser 514 nm was used to study the average bonding structure of nanotube architectures and their component bundles. The structures of individual nanotubes were probed by conventional and high-resolution transmission electron microscopy (TEM) measurements in Philips CM 12 and JEOL JEM 2010 electron microscopes, respectively. Spatially resolved energy-dispersive X-ray spectroscopy (EDX) was also carried out to reveal the catalyst location along the tubes and other local compositional variations.

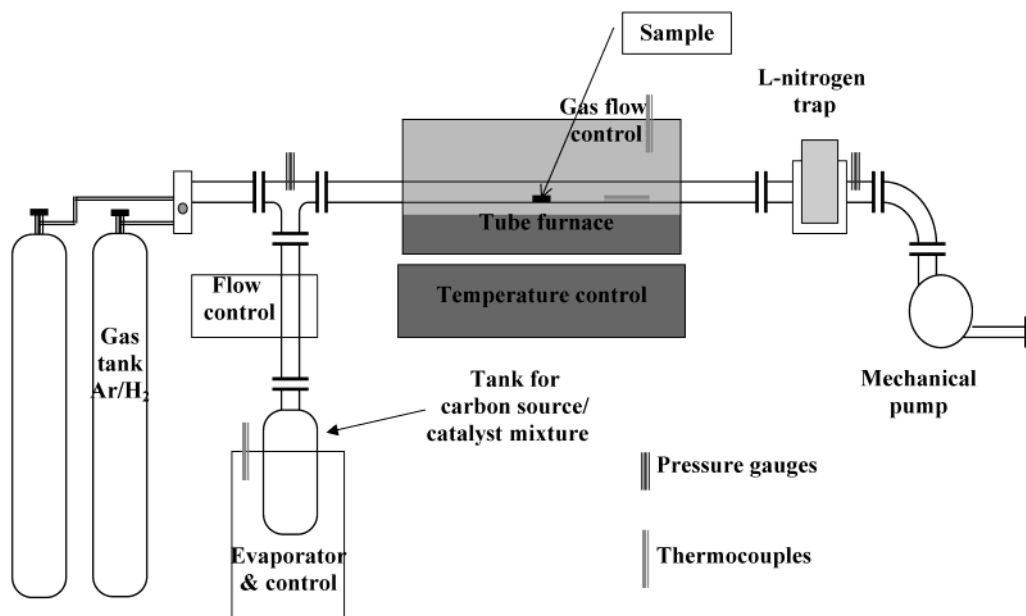


**Figure 2.** Schematic sketch of the CVD apparatus consisting of a silica tube furnace connected to a vacuum system. The heated canister used to store and deliver the catalyst–precursor mixture into the tube is also shown.



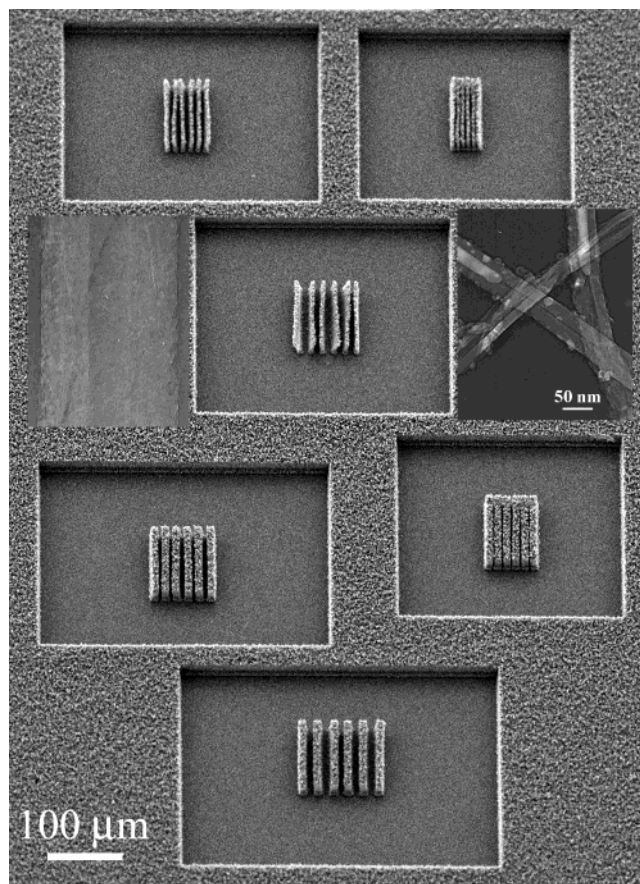


**Figure 3.** SEM micrographs showing platelets of vertically aligned carbon nanotube arrays grown on small rectangular silica islands on silicon. There is no observable growth on silicon surfaces. The platelet cross sections are  $\sim 5$ – $10$ - $\mu\text{m}$  wide and  $100$ - $\mu\text{m}$  long and are separated by 5, 2, 10, 5, 2, and  $10$   $\mu\text{m}$  from the top left to the bottom array sets, respectively. Arrays with larger separation and smaller thicknesses tend to bend at the top, compared to those that are tightly packed and thick, which are straight from end to end. The left inset shows a HRTEM image of the MWNTs grown by our process. The tubes sometimes contain Fe particles in their cavities (right inset).

### 3. Results

**3.1. Shape-Controlled Nanotube Blocks.** Figure 3 shows a striking example of platelets comprised of aligned nanotubes selectively placed on preselected sites. This result shows that highly aligned nanotubes grow readily on the  $\text{SiO}_2$  patterns in a direction normal to the substrate surface, and the selectivity is retained down to micrometer-sized  $\text{SiO}_2$  templates. No nanotube growth is observed on pristine Si surfaces or on the native oxide layer. In the center of boxlike regions defined by nanotube walls, micrometer-sized platelike blocks of vertically oriented nanotubes are grown from the underlying  $\text{SiO}_2$  pattern. Within each block, the nanotubes are highly oriented and densely packed. The primary differences between the six platelike array sets shown in Figure 3 are the separation between individual

blocks and the thickness of the platelets. The height of these blocks can be precisely controlled in the range of  $\sim 10$ – $100$   $\mu\text{m}$  by adjusting the deposition time. These oriented nanotube blocks could be attractive for use as structural reinforcements in composites.

TEM measurements show that the nanotubes constituting the architectures shown above are multiwalled (Figure 3, left inset). Many nanotubes contain Fe nanoparticles (identified by EDX) inside the hollow cavity of the nanotubes (see example in right inset in Figure 3). In some tubes, the degree of graphitization observed is lower than multiwalled tubes produced by the arc-discharge method. This is seen from the discontinuity of fringes in the HRTEM micrograph (left inset) arising from folded basal planes constituting the nanotube walls. But for these subtle differences noted in isolated instances, our multiwalled tubes are similar to those produced by other methods. This is verified by Raman spectra from our tubes showing D/G ratios of  $\sim 1/3$ , in good agreement with typical values reported for multiwalled nanotubes.<sup>25</sup>

In addition to the platelet blocks shown, one can build other shapes (e.g., circular, square, triangular, rectangular, trapezoidal) by designing the  $\text{SiO}_2$  substrate pattern accordingly. Figure 4a–e shows examples of nanotube blocks of different shapes created by lithographic chiseling of the silica templates. In all the cases, the nanotube blocks inherit the shapes of the  $\text{SiO}_2$  micropatterns on the substrate. We can obtain blocks of ordered nanotubes of predetermined shapes that are as long as several hundreds of micrometers by merely extending the growth time. Only the in-plane dimensions of silica templates determine the number of tubes in each block (e.g., pillar) and the lateral separation between the blocks, for the length-scale regime investigated. We note that there is no nanotube growth observed from the sidewalls of the  $100$ -nm-thick silica islands used in these experiments. Using thicker silica features results in in-plane growth of nanotubes from the sidewalls, as described later in section 3.3.

The nanotube blocks remain attached to the substrate even for nanotube lengths greater than hundreds of micrometers, indicating good adhesion between the nanotubes and the substrate. We note that the constituent nanotubes within each block respond in a coordinated fashion (e.g., bending during growth), suggesting that the nanotubes are held together within each geometrical block by coordinated van der Waals-type attraction. The nanotube blocks (e.g., fibers), however, can be detached from the substrates by vigorous ultrasonic agitation and can be manipulated individually.

**3.2. Porous Nanotube Membranes.** Our approach can be used to build porous nanotube films with a high degree of control over pore size, shape, and separation. This is illustrated in Figure 5, which shows examples of nanotube films with regular arrays of pores with different sizes, shapes, and configurations. These architectures are obtained by using a template with a silica film (on which nanotubes grow) with holes of different shapes etched at different locations all the way through to the Si substrate (no growth)—that is, the negative pattern of the one used to make free-standing

(22) Zhang, Z. J.; Wei, B. Q.; Ramanath, G.; Ajayan, P. M. *Appl. Phys. Lett.* **2000**, *77*, 3764–3766.

(23) Wei, B. Q.; Vajtai, R.; Jung, Y.; Ward, J.; Zhang, R.; Ramanath G.; Ajayan, P. M. *Nature* **2002**, *416*, 495–496.

(24) Drotar, J. T.; Wei, B. Q.; Zhao, Y. P.; Ramanath, G.; Ajayan, P. M.; Lu, T. M.; Wang, G. C. *Phys. Rev. B: Condens. Matter Mater. Phys.* **2001**, *64*, 125417.

(25) Benoit, J. M.; Buisson, J. P.; Chauvet, O.; Godon, C.; Lefrant, S. *Phys. Rev. B: Condens. Matter Mater. Phys.* **2002**, *66*, 073417.

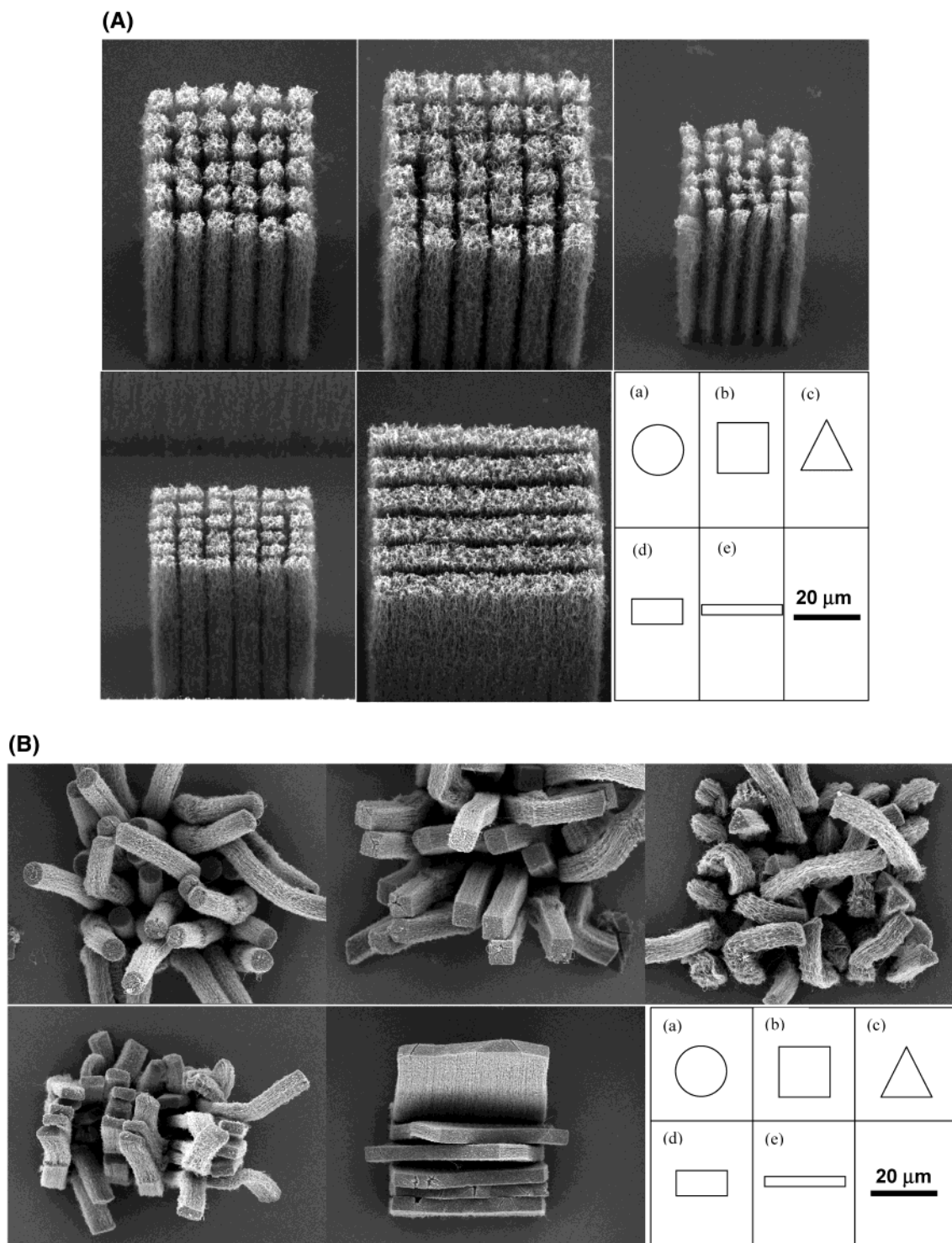


**Figure 4.** Aligned nanotube arrays grown from five differently shaped silica patterns, resulting in five different pillar cross sections: (a) circular, (b) square, (c) triangular, (d) rectangular, and (e) platelike. These results demonstrate the excellent shape control of the pillar cross sections. Nanotubes within each micropillar are highly aligned with respect to each other. Short pillars (ca. tens of micrometers shown in A) are straight, while the longer ones (ca. hundreds of micrometers shown in B) are more flexible.

nanotube blocks shown in Figures 3 and 4. Figure 6 shows examples of three pairs of positive and negative patterns that were used to generate nanotube pillars or nanotube membranes with pores at corresponding locations. This method is attractive for creating membranes with a hierarchy of pore sizes for applications such as molecular sieving and catalysis. The smallest pore size possible is the average separation between adjacent nanotubes ( $\sim 50$  nm)<sup>24</sup> or the size of the

nanotube hollow itself.<sup>26</sup> The shape and separation of the larger pores will be determined by the feasibility of lithographically chiseling silica templates of corresponding shapes and separations. The growth features shown in Figures 3–5 illustrate the excellent control over the placement at desired locations and the inheritance of

(26) Smith, B. W.; Monthieux, M.; Luzzi, D. E. *Nature* **1998**, 396, 323–324.



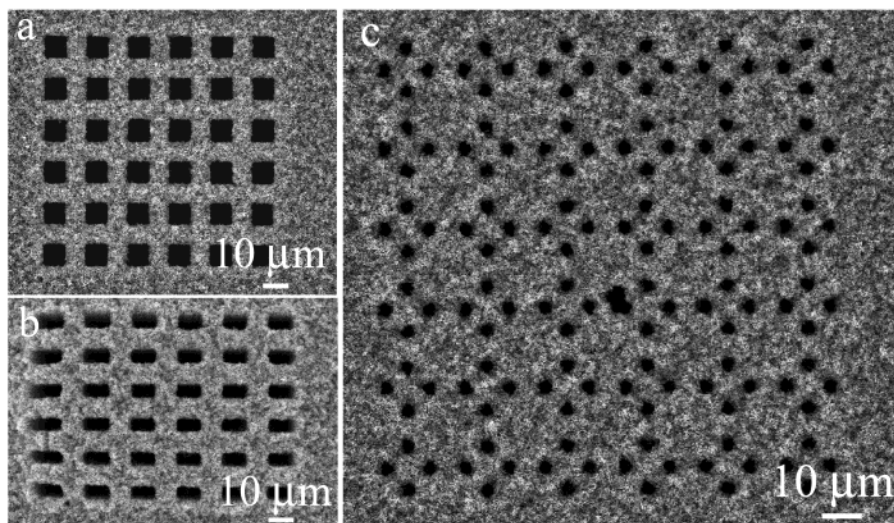


**Figure 5.** Representative micrographs showing  $\sim 50$ -nm-thick nanotube films with pores of different sizes and shapes: (a) square arrays, (b) rectangles, and (c) high-density arrays of pores placed at selected locations and separation distances. Pores shape, size, and density are controlled by using a silica template with holes of corresponding shapes, sizes, and separations, etched all the way to the Si substrate surface.

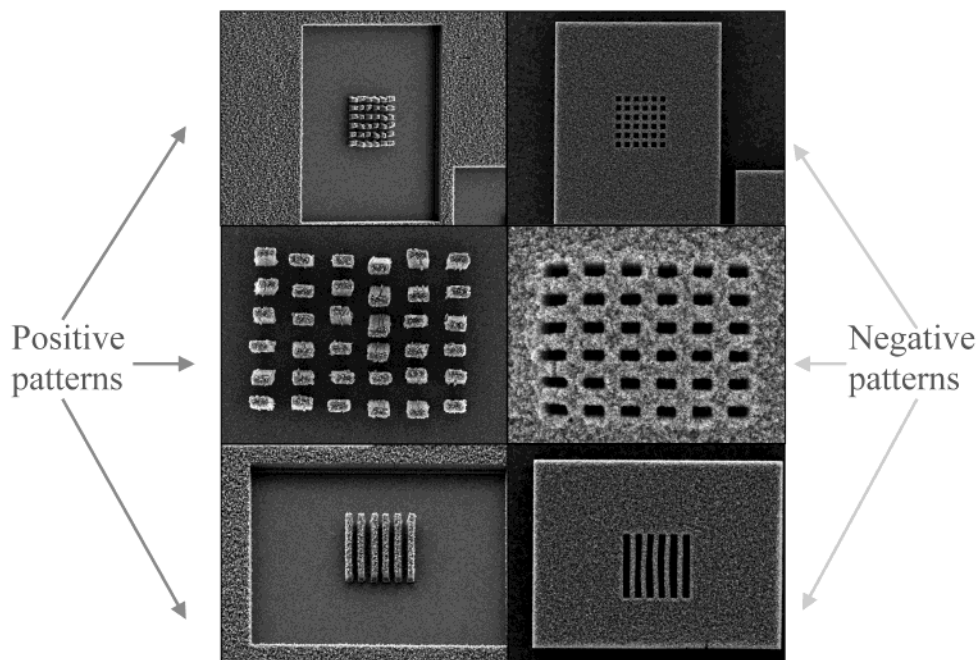


**Figure 6.** Nanotube pillars (left column) and porous nanotube membranes (right column) with square-, rectangle-, and platelet-shaped features obtained from positive and inverse patterns of lithographically chiseled silica templates. The pillars grow from silica islands patterned on silicon. The nanotube membranes with pores placed at locations corresponding to the pillars are obtained from inverse silica patterns created by using the same masks, but with a negative photoresist to pattern the silica.

the underlying template pattern shape and separation.

**3.3. Multidirectional Nanotube Architectures.** In the above instances, we grew unidirectionally oriented nanotube architectures, that is, perpendicular to the substrate surface, by keeping the thickness of silica templates below 100 nm. By using significantly thicker (e.g.,  $5\text{--}8\ \mu\text{m}$ ) silica islands of different top- and cross-sectional shapes, we are able to grow nanotube blocks oriented in multiple directions, including those in the plane of the substrate surface. For instance, we can realize nanotube growth in mutually orthogonal directions by using templates consisting of deep-etched trenches (drilled all the way to the silicon substrate), separating several micrometers-tall  $\text{SiO}_2$  towers or lines. Figure 7 showing vertically *and* horizontally (with

respect to the substrate surface) aligned nanotube arrays adjacent to each other provides an excellent example that demonstrates this concept. Also note that the placement of nanotubes is in two orthogonal directions parallel to the substrate plane itself.

We are also able to create structures where the nanotubes with oblique inclinations, (that is, neither orthogonal nor planar with respect to the substrate plane) by using deep-trench templates with inclined silica surfaces. Figure 8 shows illustrative examples where nanotubes grow normal to the walls of such circular trenches, resulting in membrane-like iris-shaped structures having the shapes of open-truncated cones. These figures also show the flexibility of our approach to obtain radially oriented nanotubes in the

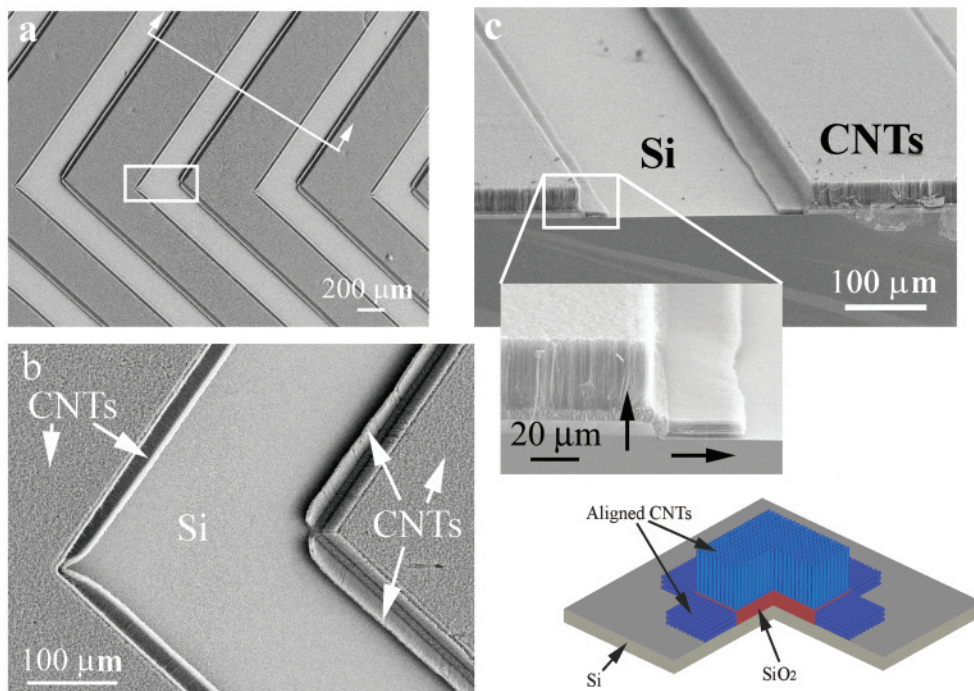


**Figure 7.** (a) Nanotube bundles oriented in both vertical and horizontal orientations grown simultaneously on a template with deep, etched trenches that separate 8.5- $\mu\text{m}$ -high  $\text{SiO}_2$  islands on Si. (b) A high-magnification view of the area marked with a white box in (a). (c) Cross section of the specimen cut along the line shown in (a). Inset shows a higher magnification image that shows the orthogonal configuration of arrays. The length of the nanotubes in both vertical and horizontal directions is  $\sim 60 \mu\text{m}$ . A schematic representation of the nanotube array growth in two mutually orthogonal directions, as seen in the images, is also shown (bottom right).

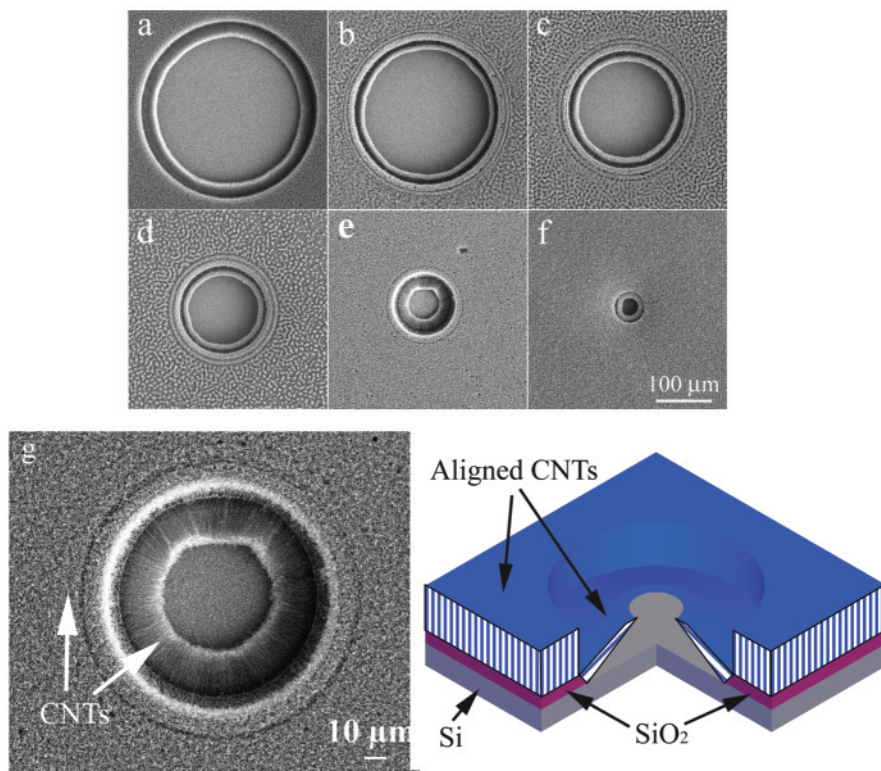


**Figure 8.** SEM micrographs of free-standing membrane structures of aligned nanotubes with the shape of truncated cones. The membrane width, inclination, and the size of the opening can be controlled by the pattern diameter, the angle of trench wall, and growth time. Typical examples of structures with different cone angles and opening sizes are shown in parts (a)–(f), for pattern diameters of 300, 250, 200, 150, 100, and 50  $\mu\text{m}$ , respectively. (g) shows an enlarged view and a schematic sketch of a 100- $\mu\text{m}$ -diameter structure shown in (e) to demonstrate the geometry of the nanotube membrane in this three-dimensional architecture.

entire spectrum of in-plane orientations on the substrate plane. We have been able to produce such structures with different diameters, cone angles, sizes of opening,

and film thicknesses by tailoring the pattern dimensions and growth time (to control nanotube length). Similarly, complex shapes of nanotube architectures can be gener-



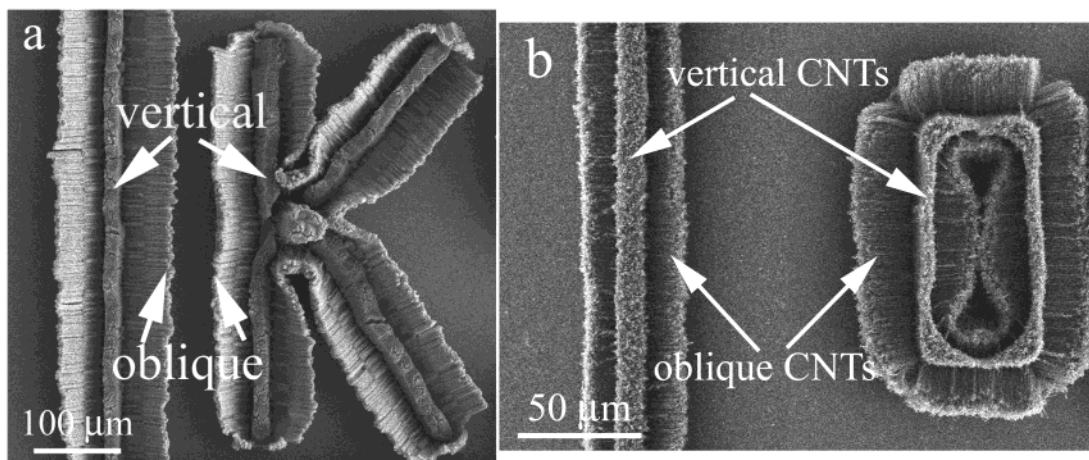


**Figure 9.** Complex architectures comprised of nanotube bundles with multiple orientations placed close to each other. Example structure showing vertically aligned nanotubes along with nanotubes making (a) large and (b) small inclination angles with respect to the substrate surface. Such structures are grown from micrometer-sized silica template surfaces of different inclinations shaped by lithography and etching.

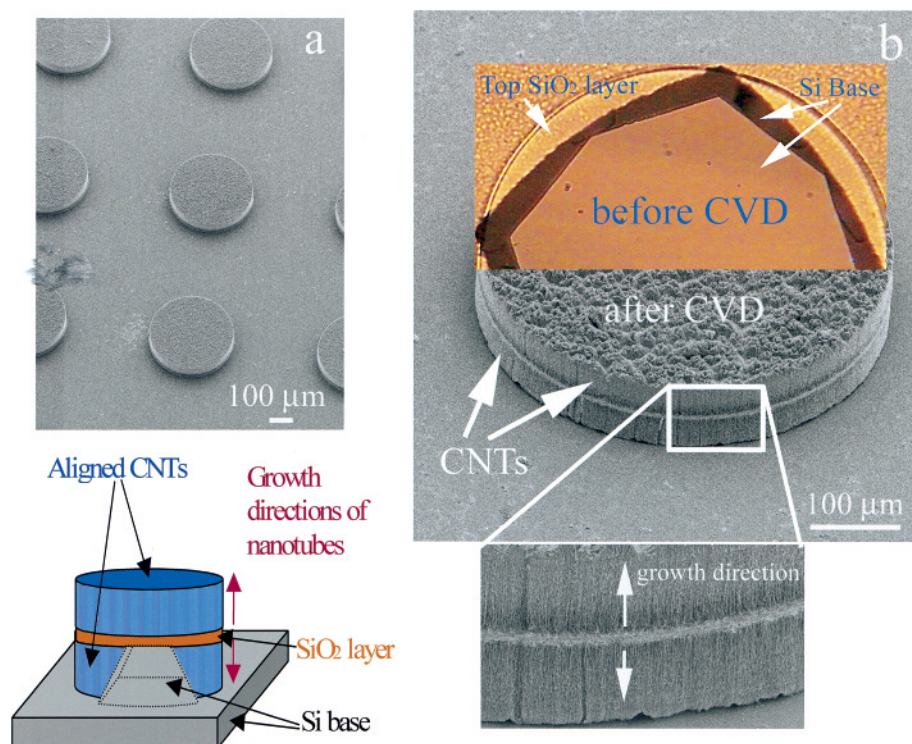


**Figure 10.** (a) A low-magnification SEM image showing a bilayer of aligned carbon nanotubes grown at a  $180^\circ$  angle with respect to each other (up and down) from the top and bottom surfaces of a circular  $\text{SiO}_2$  layer suspended on Si base pillars. The two growth directions from the  $\text{SiO}_2$  surfaces (inset) and a schematic illustration of nanotube bilayer growth are also shown. (b) An optical micrograph showing the  $\text{SiO}_2$  layer (transparent) on the silicon base pillar (opaque). This pattern suspended  $\text{SiO}_2$  templates with two exposed surfaces are generated by undercutting the silica layer, into the Si, during deep etching ( $40\text{--}50\ \mu\text{m}$ ).

ated by using silica templates of corresponding shapes. Figure 9 shows an example of one such structure with nanotube bundles of multiple orientations placed at close proximity. We note again that nanotubes grow only from surfaces whose smallest characteristic sizes are  $>100\ \text{nm}$ .

**3.4. Nanotube Multilayers.** Selective nanotube growth on  $\text{SiO}_2$  in a direction normal to the surface can also be harnessed to grow multilayer nanotube architectures. Figure 10 shows two layers of nanotubes, which grow in two opposite directions (up and down) from a suspended  $\text{SiO}_2$  layer with bottom and top surfaces exposed. The suspended silicon oxide was

generated on the silicon base pillar by deep etching ( $40\text{--}50\ \mu\text{m}$ ) of Si, undercutting the silica layer. An example of the  $\text{SiO}_2/\text{Si}$  structure is shown in Figure 10b. The circle-shaped transparent layer is the silica membrane, and the darker region shows the silicon pillar supporting it. By increasing the thickness of the suspended  $\text{SiO}_2$  layer to thicknesses  $>2\ \mu\text{m}$ , we can obtain multilayers as well as orthogonally oriented nanotube architectures in one CVD step, as demonstrated in Figure 11. The thickness dependence of whether we obtain laterally oriented nanotubes from the suspended membranes underscores the scaling effect of nanotube growth described in the previous sections.

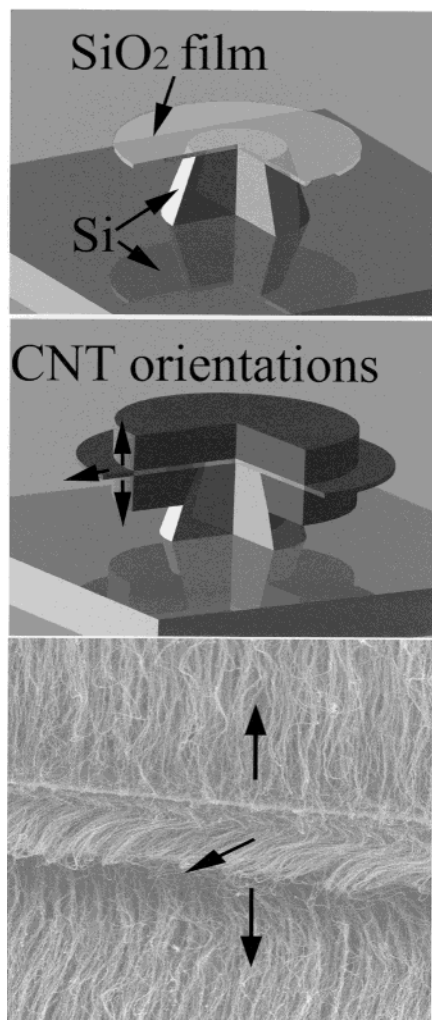


**Figure 11.** SEM micrograph and schematic sketches showing simultaneous multilayer and multidirectional growth of oriented nanotubes from a 2- $\mu\text{m}$ -thick  $\text{SiO}_2$  layer suspended on deep-etched Si pillars. Top: a schematic sketch of the substrate with a thick layer of  $\text{SiO}_2$  suspended on Si base before CVD. Middle: schematic of the nanotube growth on the suspended  $\text{SiO}_2$  layer in three orientations. Bottom: SEM micrograph showing the aligned CNTs in three directions marked by arrows.

#### 4. Discussion

Our nanotube growth process used to construct architectures described above is based on delivery of catalyst from a metal-organic precursor, ferrocene, from the vapor phase. The unique features of this process are substrate selective growth on silica—in exclusion to silicon, and vertical orientation of the nanotubes with respect to silica surfaces. Catalyst delivery via decomposition of metal-organic molecules allows selective deposition and activation<sup>22,27</sup> on different surfaces because of corresponding differences in chemical reactivities and kinetic pathways. In our case, nanotubes grow from Fe particles formed by selective decomposition of ferrocene on silica,<sup>22</sup> indicated by our TEM and EDX results showing the presence of Fe particles inside the nanotubes. This result is consistent with earlier reports which show that Fe catalyzes

nanotube growth.<sup>16</sup> The reason for lack of activation of an Fe-based catalyst for nanotube growth on silicon is yet to be determined. However, preliminary TEM and X-ray photoelectron spectroscopy measurements show that ferrocene reacts with silicon to form a Si-containing compound, which may not favor nanotube growth.<sup>28</sup>

Vertically aligned nanotubes have been grown by several researchers on metal-catalyst templates.<sup>12–18</sup> While the reason for aligned nanotube growth is not yet understood, a plausible driving force is the free energy reduction due to coordinated growth of nanotubes held together by intertube attraction resulting from van der Waals-type forces along the nanotube length. Our results showing a strong influence of the silica template dimensions on nanotube growth supports this view. As described in sections 3.1 and 3.3, nanotubes do not grow from silica sidewalls that are <100-nm-thick silica sidewalls. We can also reproduce this scaling effect in directions perpendicular to the substrate surface: no vertical nanotube growth is observed from silica pillars with feature sizes  $\leq 100$  nm.<sup>29</sup> Instead, we obtain a thin layer of amorphous carbon film and isolated, trace amounts of random nanotubes lying on the surface.<sup>30</sup> On the basis of the above, we propose that the lack of aligned nanotube growth on small silica features is related to insufficient surface area to promote the growth of enough nanotubes in a coordinated fashion to support each other. Further studies are required to understand the mechanism(s) for this scaling effect.

A key advantage of selective growth enabled by in situ vapor-phase catalyst delivery is that it obviates the need for *pre-deposition* and patterning of catalyst films or particles—generally required for CVD growth of nanotubes.<sup>14–17</sup> This not only simplifies template preparation by decreasing deposition and patterning steps but also endows freedom for process optimization<sup>31</sup> and extension of our strategy to growth of other nanostructures through manipulation of catalyst-precursor chemistry. The power of combining selective growth and lithographic chiseling is underscored by that fact that simultaneous multidirectional growth of oriented nanotubes demonstrated here has not been shown by any other template growth method to date. Another unique feature of our growth method is that it is easily integrated with Si- $\text{SiO}_2$  technology, which is an integral part of current microscale devices and electromechanical systems. As mentioned earlier, we also envision our growth strategy to enable the realization of nanotube architectures for diverse applications such as porous membranes for molecular separation and pillar structures for electro-mechanical actuation and sensing or structural reinforcements in composites.

#### 5. Summary

In summary we describe a powerful method for assembling carbon nanotubes on planar substrates to build highly organized one- to three-dimensional archi-

(28) Jung, Y. J.; Wei, B. Q.; Vajtai, R.; Ajayan, P. M.; Homma, Y.; Krabhakaran, K.; Ogino, T., unpublished.

(29) Jung, Y. J.; Wei, B. Q.; Ramanath, G.; Ajayan, P. M., unpublished.

(30) Cao, A.; Wei, B. Q.; Jung, Y.; Vajtai, R.; Ajayan, P. M.; Ramanath, G. *Appl. Phys. Lett.* **2002**, *81*, 1297–1299.

(31) Zhang, Z. J.; Wei, B. Q.; Ward, J.; Vajtai, R.; Ramanath, G.; Ajayan, P. M. *Adv. Mater.* **2001**, *13*, 1767–1770.

(27) Wei, B. Q.; Vajtai, R.; Zhang, Z. J.; Ramanath, G.; Ajayan, P. M. *J. Nanosci. Nanotechnol.* **2001**, *1*, 35–38.



tructures. The growth of aligned multiwalled nanotubes in patterns and in multiple directions on lithographically machined templates of oxidized silicon surfaces occurs in a single process, carried out through gas-phase precursor and catalyst delivery. Nanotubes grow normal to, and selectively on, silica, inheriting the topography of the substrate templates. This enables the fabrication of a wide variety of organized architectures comprised of nanotubes arranged in differing complexity, shapes, density, dimensions, and orientations for applications. Model structures we have grown, for example, microfibers and membranes consisting of highly aligned nanotubes, could find use in many applications such as

nanocomposites, fluidic channels, electromechanical actuation, and electrode systems. The fabrication method described here is versatile and is easily scalable to enable commercial production with the aid of fabrication techniques commonly used in microelectronics.

**Acknowledgment.** This work was supported by the Office of Naval Research under Grant N00014-00-1-0250 and by the interconnect fc-ny (Focus Center—New York) at RPI, which is funded by MARCO and New York State.

CM0202815